

# Computation of Holdups in Fluidized and Trickle Beds by Computer-Assisted Tomography

Apostolos Kantzas

Novacor Research & Technology Corp., Calgary, Alberta, Canada T2E 7K7

*A fourth-generation X-ray computer-assisted tomography (CAT) scanner was used for the study of fluidized and trickle beds. A variety of exploratory experiments were performed, and images of density and holdup were obtained in three dimensions as a function of time. The gas/solid fluidized beds were glass bead/nitrogen and polyethylene/nitrogen systems. The trickle bed was a glass bead/nitrogen/water system. The algorithms presented can be used to determine holdup from X-ray absorption data. These algorithms—extensions of similar algorithms used for the calculation of fluid saturations in porous media—are applied on data of CAT scanner images as they are generated by the scanner and after they are transferred to a workstation. The results of the presented tests demonstrate how detailed holdup calculations can be performed in a chemical reactor. Radial and longitudinal variances of the holdup can be easily defined. The proposed algorithms can assist in the design of chemical reactor prototypes.*

## Introduction

Solids motion plays important roles in various applications of fluidized-bed technology. Among these applications are the enhancement of heat and mass transfer, material processing, catalytic cracking, particle sedimentation, and others. A better understanding of solids movement is often crucial to the fulfillment of the promise of these fluidization theories. Despite its importance, there is little information on *in-situ* measurements of particle motion in fluidized beds.

In addition to the motion of solids, the relative position of solids and fluids is also very important. The concept of holdup (or void fraction) is used to describe the volumetric distribution of fluids in a bed. In a fixed bed, the holdup is constant. In a fluidized bed, however, the holdup varies with position and external conditions. In the case of a trickle bed, the holdup of the individual phases can also vary with position and external conditions.

In most cases, in lack of any better values, the holdup is considered to be constant. Up until now there was no method that could help evaluate the holdup in a fixed or fluidized bed *in three dimensions* with any degree of spatial resolution. This is now changed with the use of computer-assisted tomography.

## Literature Survey on Flow Visualization

Although X-ray CAT scanning has not been used for the monitoring of fluidized beds, a number of X-ray and gamma-

ray monitoring techniques have been incorporated for performance monitoring both in the laboratory and in the plant. CAT scanning (or CT scanning) has been identified as a valuable method for the noninvasive measurement of material properties and the determination of fluid saturations in porous media (Kantzas et al., 1992). Very extensive research was conducted in this area, and literature reviews revealed that CAT scanning can help understand reservoir properties and oil recovery mechanisms (Kantzas, 1990; Kantzas et al., 1992).

Single bubble measurements were made using a X-ray source at a speed of 8 frames/s as reported by Rowe and Matsuno (1970). The minimum fluidization velocity was measured, and the size and shape of rising bubbles were measured as a function of time. Rowe et al. (1979) studied the gas discharge from an orifice into a gas-fluidized bed. Various powders were fluidized by air in a 15.2 cm dia. vessel fitted with a porous plate distributor through the center of which was a pipe through which secondary air could be blown independently. The mode of entry of this secondary air was observed by taking ciné photographs of exposure time 0.001 s at 50 frames/s. Conditions at air velocities up to 70 m/s through pipes up to 1.6 cm dia. were observed in this way. In a similar study, Rowe and MacGillivray (1980) found that in small diameter cylindrical beds (up to 15 cm in dia.) axisymmetric annular flow is not established up to velocities of 1 m/s.

Fincke et al. (1980) described a gamma-ray tomographic

densitometer for the measurement of density distribution in two-phase flow. Results based on real and simulated phantoms show a density accuracy of 2% of scale.

Lin et al. (1985) presented a radioactive particle tracking facility for measurement of solids in motion in gas-fluidized beds. A radioactive tracer particle, dynamically identical to the solid particles to be studied, was mixed with the solids in the bed. The gamma radiation from the tracer was continuously monitored by a large number of scintillation detectors located around the bed, providing information on the tracer's instantaneous location. The authors found that for a bed with uniform air distributor plate the existence of two counterrotating toroidal vortices was shown. The vortices' relative sizes and strengths vary with the fluidizing velocity.

MacCuaig et al. (1985) and Seville et al. (1986) presented the first tomographic technique for monitoring fluidized beds. A first-generation gamma-ray scanner was introduced and used for the determination of density profiles in glass bead/air systems. The authors were discouraged from using X-rays because of the inherent problems of a X-ray beam (polychromatic, soft) and the facts that they aimed at creating a system for industrial use. They found that their scanner could provide time-averaged density profiles for the fluidized bed, but the scanner is very slow. The authors reported that it takes between 6 and 7.5 hours per scan.

In Yates et al. (1990), a freely bubbling fluidized bed containing horizontal banks of tubes was observed by X-rays. They performed experiments where number of rows of tubes, the distance between them, the distance of the first row of tubes above the distributor and the fluidizing gas velocity were all varied, the size distribution of bubbles rising through the tube banks being recorded on ciné film for subsequent frame-by-frame analysis. Based on their observations they developed a correlation for the breakage rate, which was combined with an expression for bubble growth to give predictions of bubble size at any point in a bed fitted with tubes. Good agreement was achieved.

Modi et al. (1990) used a second-generation EMI 5005 full-body scanner to study two-phase flow in a pipe. The local void fraction was measured in turbulent two-phase flow through a 3.75 cm dia. pipe. The void fraction data were time-averaged over a period of 30 s. Steady-state phenomena can therefore be monitored accurately.

A novel application of computer-assisted tomography was presented by Lutran et al. (1991). X-ray CAT scanning was used for the visualization of liquid distribution in trickle beds. A series of visualization experiments were presented where flow patterns were recorded as a function of the liquid flow rate, the size of particles, the type of liquid inlet distributor used, and surface tension. The liquid phase was doped with barium bromide to increase its absorption index. The work presented here extends the work of Lutran et al. (1991) by providing a method of quantifying the observations of the aforementioned authors. The presented approach is analog to the determination of properties and fluid saturations in reservoir rocks. The equivalent reservoir rock methods are presented in detail elsewhere (Vinegar and Wellington, 1987; Kantzas, 1990).

The above literature demonstrates how one can image holdups for systems similar to a chemical reactor. The techniques vary widely. Speed may be gained by some methods, but three-dimensional resolution is lost. The fast CAT scanner can pro-

duce three-dimensional resolution at reasonably fast testing times.

Although the review demonstrated that CAT applications in fixed and fluidized beds are very limited, it by no means implies that there are no other methods for holdup determination. Other methods include gravimetric, tracer and electrical conductivity algorithms (Ramachandran and Chaudhari, 1983). These methods provide volume-average values for the column and are useful if a mean holdup value is required. However, when 3-D holdup information is the objective, all these methods are inadequate.

## Experiments on Fluidized Beds

The EMI 7070 scanner was used for all the fluidized bed experiments. The scanner is a fourth-generation modified medical scanner, which has been adapted to perform scans in both vertical and horizontal direction. For the objectives of this work, the vertical scan position (horizontal gantry position) was used throughout. The scanner gantry in its horizontal position is shown in Figure 1. Objects of up to 32 cm in diameter could be scanned in energies that could vary between 100 and 140 kVp. It must be kept in mind that as the density of the object under study increases, the size (diameter) to be scanned decreases. For example, a column of 30 cm in diameter which is packed with polyethylene can be easily scanned. A column packed with silica particles can be scanned only if it is less than 15 cm in diameter. The gantry rotates with the aid of a crane (located over the scanner), and a safety pin holds the bearings locked in the desired position. Although only two positions can be locked at present, the gantry could be locked

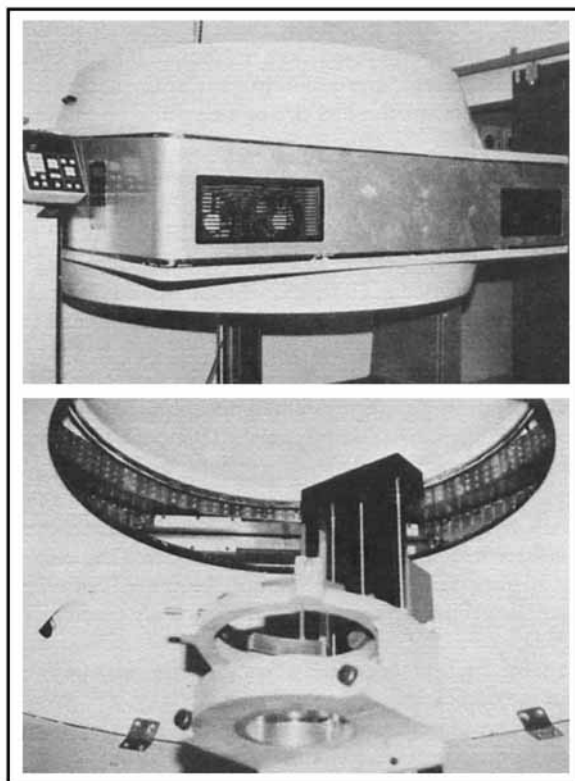


Figure 1. EMI 7070 CAT Scanner.

in any desired angle, provided that the pin design is modified. Also in Figure 1, the body of the precision sample holder device can be seen. Objects can be moved in and out of the gantry with a 0.001 cm precision when sequential scanning is desired. Figure 1 also shows the top of the positioning device which was designed and built for positioning of core holders, or other columns in vertical position. It takes 3 s to scan one slice of the column under study. In a gas-fluidized bed where bubbles form at a frequency of 8/s and rise with a velocity of several tens of cm/s, the image obtained through a 3 s time interval is the time-averaged, X-ray attenuation image of this cross section.

The X-ray CAT scanner measures the X-ray absorption through the linear attenuation coefficient,  $\mu$ , which is defined as:

$$\mu = (1/L) \ln(I/I_0) \quad (1)$$

where  $I$  is the transmitted intensity,  $I_0$  the incident intensity, and  $L$  the path length. The CAT scanner readings are usually reported in the form of the so-called CT number ( $CT_n$ ) defined as:

$$CT_n = K(\mu - \mu_w) / \mu_w \quad (2)$$

where  $\mu$  is the measured linear attenuation coefficient and  $\mu_w$ , the linear attenuation coefficient of water and  $K$  is a constant.

The image resolution can go down to  $0.04 \text{ cm} \times 0.04 \text{ cm}$ . The thickness of the slice can vary between 0.1–1.0 cm. As a result, a detailed map of the X-ray absorption image can be obtained. The X-ray absorption is a linear function of the bulk density which is a linear function of the gas void — fraction. Therefore, the CT scanner can provide a detailed map of the gas holdup. This map is the 3 s time-average map and, in the case of a uniform fluidized bed, it should have a constant value. Consequently, any nonuniformities in the gas holdup due to the design of the bed or the operating conditions can be detected.

The first set of experiments was run using a gas/solid fluidized bed which consisted of glass beads fluidized by the flow of nitrogen, as shown in Figure 2. A distributor plate with a long orifice in the center was used for the distribution of nitrogen flow. The central orifice, when in operation, was used to create a large nitrogen jet. The column was scanned at two different levels: one below and one above the tip of the central orifice. Different nitrogen pressure values were applied, and the bed response was recorded at a resolution of  $0.04 \text{ cm} \times 0.04 \text{ cm} \times 0.5 \text{ cm}$ . In a second run with the same bed, nitrogen was pushed through at constant pressure, and the whole column was scanned from top to bottom. Transverse images were obtained directly while longitudinal image reconstruction of the fluidized beds was obtained by manipulating the slice data, using software developed in house for the analysis of reservoir core samples. The experimental parameters are given in Table 1.

In a second set of experiments, polyethylene was used as the solid in the same apparatus. The bed was fluidized at constant pressure, and sequential scans were taken at the same resolution. The polyethylene was taken from our technical-scale reactor (TSR) with a plaque density of  $926 \text{ kg/m}^3$ . A series of standards of known density were used to determine a density

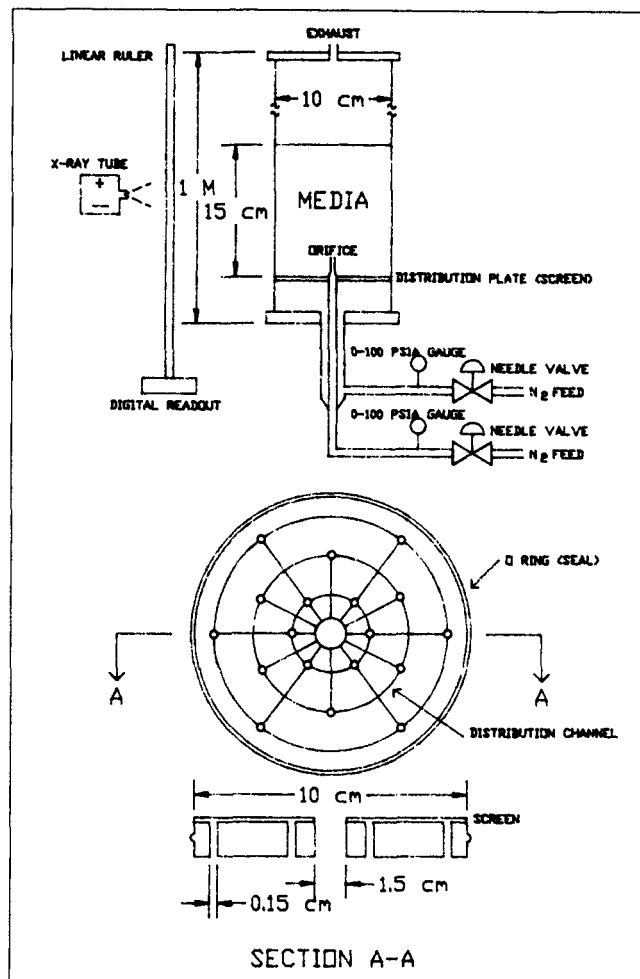


Figure 2. Experimental apparatus and distributor plate for the fluidization experiments.

vs. CT number calibration curve. For the range of densities close to the density of water, this curve is of the form:

$$\rho = 0.00101 CT_n + 1.076 \quad (3)$$

as was determined by a regression analysis of calibration data (see Figure 3). Then, the bed density was translated to gas holdup by using the equation:

$$\epsilon_g = 1 - (\rho / \rho_{PE}) \quad (4)$$

Thus, the gas holdup was calculated for every voxel of the bed, that is, at the same resolution as the CT number data.

Table 1. Experimental Parameters

Bed diameter	10 cm
Bed height	15 cm
Column height	100 cm
Inlet gas pipe diameter	1.5 cm
Glass bead particle size	20–30 mesh
Polyethylene particle size	0.04 cm
Gas inlet pressure	0, 170, 308 kPa
Gas flow rate	0, 24.25, 38.1 SLPM

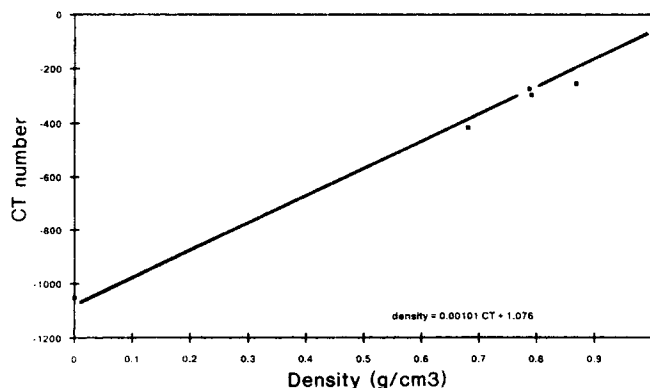


**Figure 3. CT number vs. density calibration line for the polyethylene/nitrogen fluidized bed.**

### Discussion of Fluidized-Bed Tests

Figure 4 shows a series of CT number images taken at various points in the glass bead/nitrogen fluidized bed. The first two rows of images are taken prior to fluidization. The ones with the hole in the middle are images taken below the tip of the orifice and the rest taken over the orifice. Relatively uniform images are shown in all cases. The third row shows a series of scans over the orifice tip with the bed fluidized and the orifice flow creating a jet. The CT images show the degree of mixing in these slices. Near the wall the CT numbers are like the images

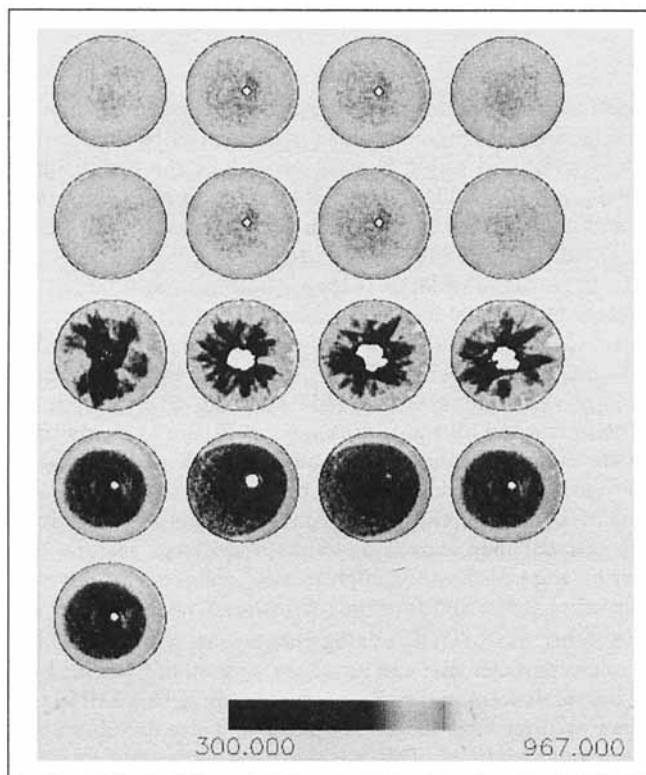


**Figure 4. CAT scanner images of the glass beads/nitrogen fluidized bed.**

First two rows are images from the bed prior to fluidization. Third row shows images while channeling is created over the extended orifice during fluidization. The last two rows show images of the column settling after fluidization ends.

prior to fluidization. This is an indication that there is not any significant gas flow and no good mixing. Finally, the bottom rows show CT images of the fluidized bed after the gas flow stops. The bed does not settle back to its prefluidization condition, as expected, and there is a definite segregation between the zones where good mixing took place as opposed to the areas where mixing did not take place. It must be stated that the images are by no means general. They are just taken to illustrate that a contrast in CT numbers can lead to observations about mixing in a fluidized bed.

In the figure that follows, the whole bed is scanned from bottom to top. Figure 5 shows the CT images arranged by row. The first slice of the fluidized bed is right over the distributor plate. Some of the jets created from the gas flowing through the holes in the distributor plate can be seen. The column was scanned from bottom to top at a slice thickness of 0.5 cm. Twenty-three slices were obtained. The images show that, as we move to the top of the bed, the images become more uniform. As the tip of the orifice is reached (slice 10), there is a small area of high density followed by an expanding jet. There is a thin, high-density ring surrounding the expanding jet indicating a high concentration of particles surrounding the gas jet. The jet becomes wider as the top of the bed is reached. In Figure 6, the mean CT number value is plotted against the column height. The slope of the density profile changes when the tip of the orifice is reached, indicating that there is a change in the holdup distribution as a function of bed height.

The calibration curve of Figure 3 was used for the plot of

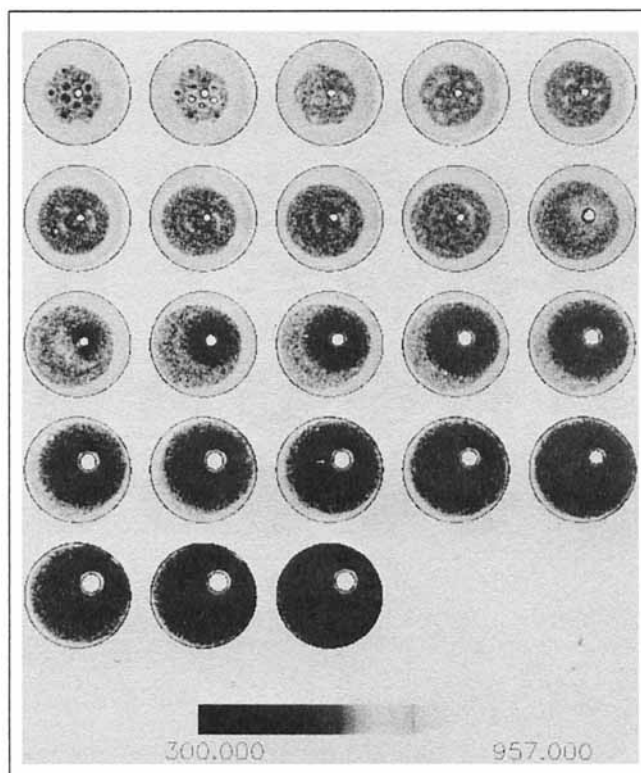


**Figure 5. Sequence of CAT scanner images for the glass beads/nitrogen fluidized bed.**

The scans are taken every 0.005 m. The arrangement is by rows with the first image taken at the distributor plate.

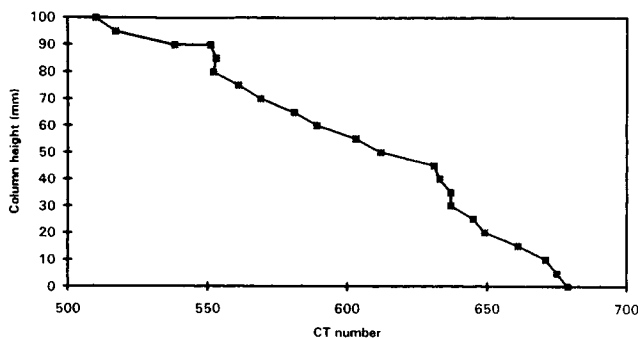


**Figure 6. Average CT number as a function of column height for the glass beads/nitrogen fluidized bed.**

the gas holdup profile in the polyethylene fluidized bed. A set of standards of known density was scanned, and their average CT numbers were plotted against their density. For the demonstration of holdup calculations, a series of tests were performed in a polyethylene/nitrogen fluidized bed. The estimated gas holdups for each one of the steps is shown in Figures 7–10. All image arrangements are by rows. Figure 7 shows the bed images prior to fluidization. The bed is quite uniformly packed with the exception of the last three slices that correspond to the top of the bed. Figure 8 shows the same column, but now fluidization has started at 170 kPa inlet gas pressure. The column shows a variety of patterns of mixing, more vigorous at the bottom and less so at the top. Forty slices were

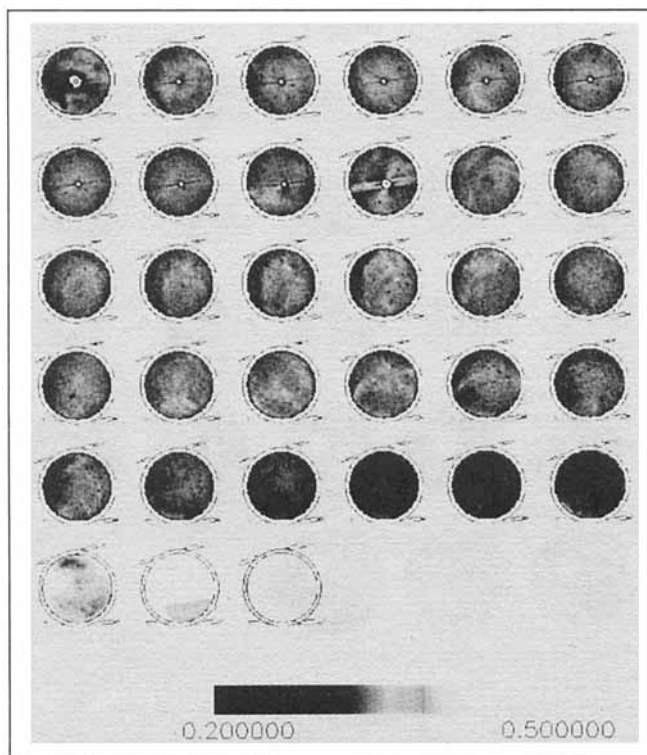


**Figure 7. Gas holdup distribution of a polyethylene bed prior to fluidization.**

Arrangement is by rows with the first image taken at the distributor plate.

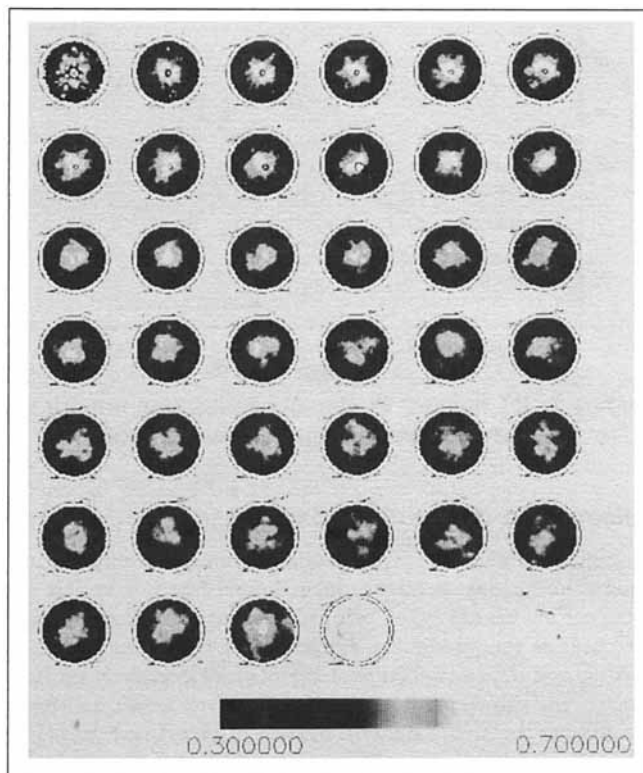


**Figure 8. Gas holdup distribution of polyethylene bed at nitrogen inlet pressure of 170 kPa (10 psig).**

Arrangement is by rows with the first image taken at the distributor plate.

taken to cover the whole bed, which are eight more than the number of slices needed to scan the bed prior to fluidization. The fluidization height is 4 cm more than the bed at initial conditions. When the pressure is brought down to zero, there is still considerable expansion of the bed as shown in Figure 9. There was a need for 35 slices to scan the bed. There is also significant radial variation in the gas holdup both at the bottom and the top parts of the fluidized bed. When the gas flow starts again at 308 kPa inlet nitrogen pressure, the corresponding bed picture is shown in Figure 10. Again significant radial holdup variations are observed. The slice averages for the aforementioned four tests are shown in Figure 11 as functions of the column height. If one had to look at this plot alone, the conclusion would have been that, except for the very bottom of the column, the fluidization is quite uniform. The three-dimensional map, however, shows a different picture. The combination of the above figures also indicates that any one-dimensional description of the column is an oversimplification.

Another way to study mixing phenomena in a fluidized bed is to use particles that can be traced separately from the bulk of the fluidized material. However, care must be taken so that these particles have the same density and size distribution of the regular particles. This was achieved in the current study by using a batch of polyethylene particles that were soaked in a NaI solution which was then let to dry. In the CAT scanner images, the NaI-tagged particles appear to be a lot denser than the untagged particles. So, in principle, one could trace the tagged particles and study mixing. This was demonstrated in a simple test. A section of the fluidized-bed column was filled

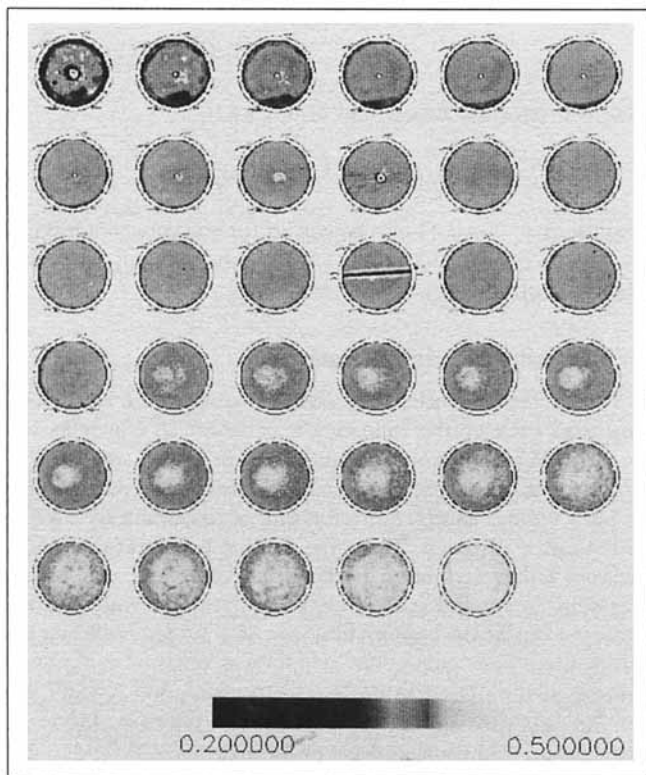


**Figure 9. Gas holdup distribution of a polyethylene bed after the end of fluidization (pressure brought down to zero).**

Arrangement is by rows with the first image taken at the distributor plate.

with the tagged polyethylene, while the rest was filled with untagged polyethylene. The column was scanned from bottom to top. Then, nitrogen was allowed to flow from the distributor plate at 170 kPa inlet pressure. The column was scanned again from bottom to top. In the area that mixing did not occur, the tagged particles did not move and were easily identified. A few high CT number particles were observed in other parts of the image indicating that vigorous mixing occurred in the central part of the column. Looking at the overall picture for the column before and after fluidization, it was found that above slice 10 there is no trace of tagged polyethylene.

The last test with the fluidized bed aimed at visualizing the change of gas holdup as a function of time in a single slice. The polyethylene column (with the mixture of tagged and untagged polyethylene) was scanned at settling condition and then at 170 kPa nitrogen inlet pressure in sequence for one-half hour. The gas holdup images are shown in Figure 12. Throughout the scanned zone, there are distinct differences among the slices. Sequences like the one of Figure 12 can be very helpful in understanding the fluidization phenomena in a particular location on the bed. It can also be noted that average gas holdups for all the slices fell within a 0.04 range.

### Determination of Holdup in Trickle Beds

Let us consider a packed bed which is dry. We define as holdup,  $\epsilon$ , the void fraction of the bed. When a liquid and a gas phase are flowing through the column, part of the void

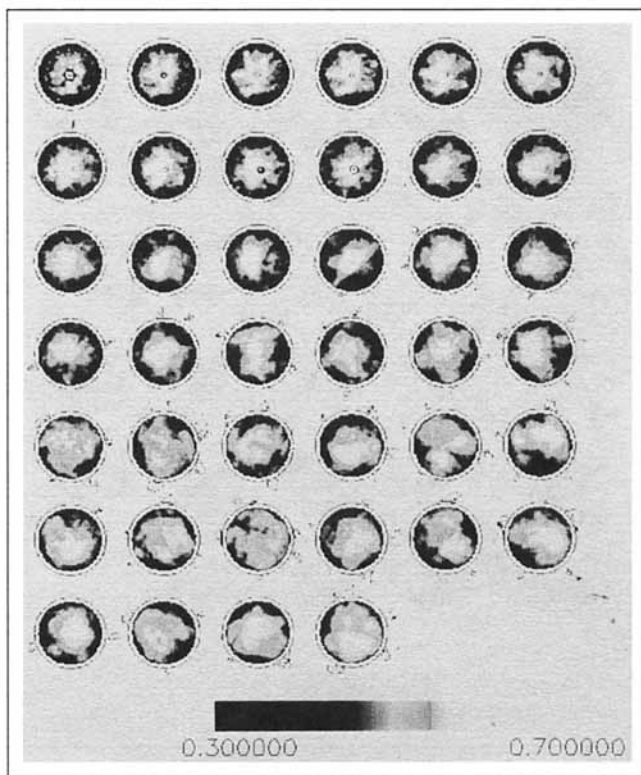


**Figure 10. Gas holdup distribution of polyethylene bed when nitrogen inlet pressure is brought up to 308 kPa (30 psig).**

Arrangement is by rows with the first image taken at the distributor plate.

fraction is occupied by the liquid and part by the gas. The liquid holdup  $\epsilon_l$ , and the gas holdup  $\epsilon_g$  must obey:

$$\epsilon_l + \epsilon_g = \epsilon \quad (5)$$

or

$$(\epsilon_l/\epsilon) + (\epsilon_g/\epsilon) = 1 \quad (6)$$

The overall X-ray absorption is the sum of the individual absorption for the components of the sample under study. As a result, if the bed is scanned dry (only gas present), then at

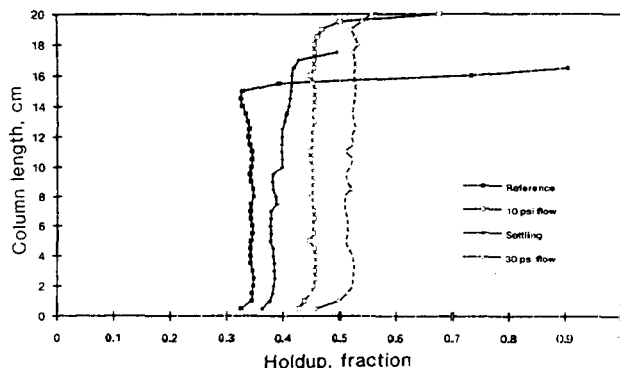


**Figure 11. Average slice gas holdups from Figures 7-10 as functions of column height.**



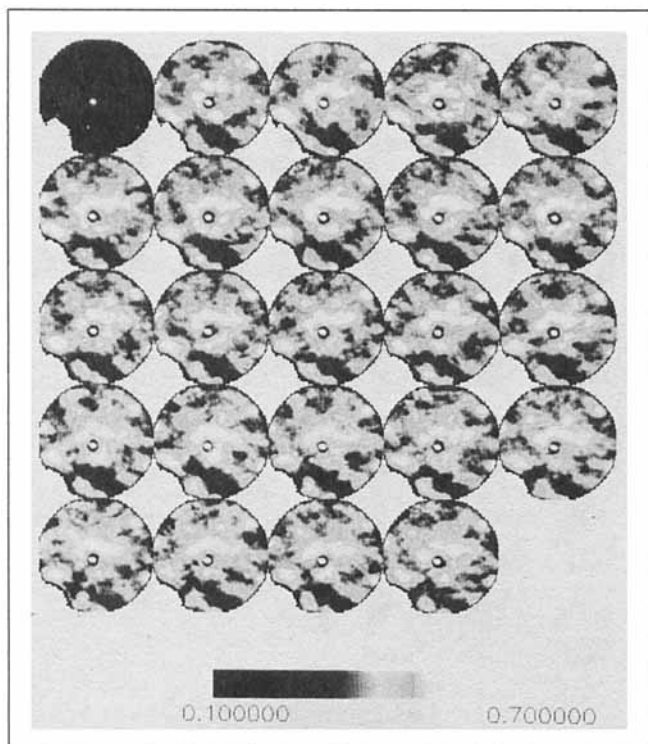


**Figure 12. Gas holdup sequence of images for the same slice starting at zero pressure (first image) and continuing at 170 kPa for one-half hour.**

any volume element or voxel, the measured CT number will be:

$$CT_{dry} = CT_{gas} \epsilon + CT_{pack} (1 - \epsilon) \quad (7)$$

where  $CT_{dry}$  is the measured CT number,  $CT_{gas}$  the CT number for the gas, and  $CT_{pack}$  the CT number for the packing. If the column gets saturated with a liquid, then the measured CT number will be:

$$CT_{sat} = CT_{liq} \epsilon + CT_{pack} (1 - \epsilon) \quad (8)$$

where  $CT_{sat}$  is the measured CT number,  $CT_{liq}$  the CT number of the pure liquid. Rearrangement of Eqs. 7 and 8 gives the equation for holdup:

$$\epsilon = (CT_{sat} - CT_{dry}) / (CT_{liq} - CT_{gas}) \quad (9)$$

when the bed is scanned with liquid and a gas present, and then the measured CT number for the mixture  $CT_{mix}$  is given by:

$$CT_{mix} = \epsilon[(\epsilon_l/\epsilon)CT_{liq} + (\epsilon_g/\epsilon)CT_{gas}] + (1 - \epsilon)CT_{pack} \quad (10)$$

by incorporating Eq. 6 in Eq. 10, one can derive:

$$CT_{mix} = \epsilon[(\epsilon_l/\epsilon)CT_{liq} + (\epsilon_g/\epsilon)CT_{gas}] + [(\epsilon_l/\epsilon) + (\epsilon_g/\epsilon)](1 - \epsilon)CT_{pack}$$

or

$$CT_{mix} = (\epsilon_l/\epsilon)[\epsilon CT_{liq} + (1 - \epsilon)CT_{pack}] + (\epsilon_g/\epsilon)[\epsilon CT_{gas} + (1 - \epsilon)CT_{pack}]$$

and incorporating Eqs. 7 and 8, one gets:

$$CT_{mix} = (\epsilon_l/\epsilon)CT_{sat} + (\epsilon_g/\epsilon)CT_{dry} \quad (11)$$

Equations 5, 9 and 11 can be solved for the determination of the holdup of each phase. The CAT scanner resolution dictates the minimum dimensions of each voxel.

## Experiment in Trickle Bed

The concepts mentioned at the previous session were demonstrated through the following experiment. A Plexiglas column, 0.045 m in diameter and 0.45 m in length, was packed with glass beads of sizes 0.4–0.6 mm. The column was scanned at 140 kVp and 28 mA every 3 mm at a resolution of 0.4 mm × 0.4 mm × 3.0 mm. Then, the column was saturated under vacuum with water and scanned again. Afterward, the column was dried again and at this point circulation of water started from the top of the column at a rate of 1.57 cm<sup>3</sup>/s. When the steady state was reached the column was scanned again from bottom to top. The EMI 7070 fourth-generation X-ray CAT scanner was used for the experiment. In each case, 150 scans were taken, and each image was an array of 320 × 320 elements. The collected images were stored in magnetic tapes, which were used to transfer the data to a SUN 4 workstation for analysis and holdup calculation. All calculations were performed at a pixel level. Slice averages are also presented.

## Discussion of Trickle-Bed Experiment

Figure 13 shows the water holdup map of forty 3 mm slices in the trickle bed. Holdup differences in each cross section can be clearly visualized. For all calculations of liquid and gas holdup, a region of interest approach was taken. The column walls and outside air were eliminated from the calculation process. The average water holdup fractions ( $\epsilon_l/\epsilon$ ) were calculated to be between 0.74 and 0.91. As can be seen from the images, the distribution of fluid holdup in the bed is not uniform despite the fact that the packing is uniform. Liquid pockets and filaments can be identified easily. Figure 14 provides a plot of the liquid gas and total holdup along the length of the bed. The flow is shown to be nonuniform throughout the bed, but more so at the top where large gas pockets exist.

The presented example is a simple demonstration of what information can be obtained by using the CAT scanner technology in association with trickle beds. The proposed method provides a tool for the quantitative estimation of holdup in the bed. The holdup values can then be used to solve for the equations of flow locally. More accurate descriptions of the hydrodynamics of the bed can be achieved. Similar information can be achieved for any two-phase system in a fixed bed.

## Conclusions

Computer-assisted tomography scanning can be successfully used for the flow visualization in two-phase fluidized bed systems. When proper calibrations are made, the CAT scanner can be used for the determination of the gas holdup in gas/solid fluidized beds. The column bulk density or the gas holdup

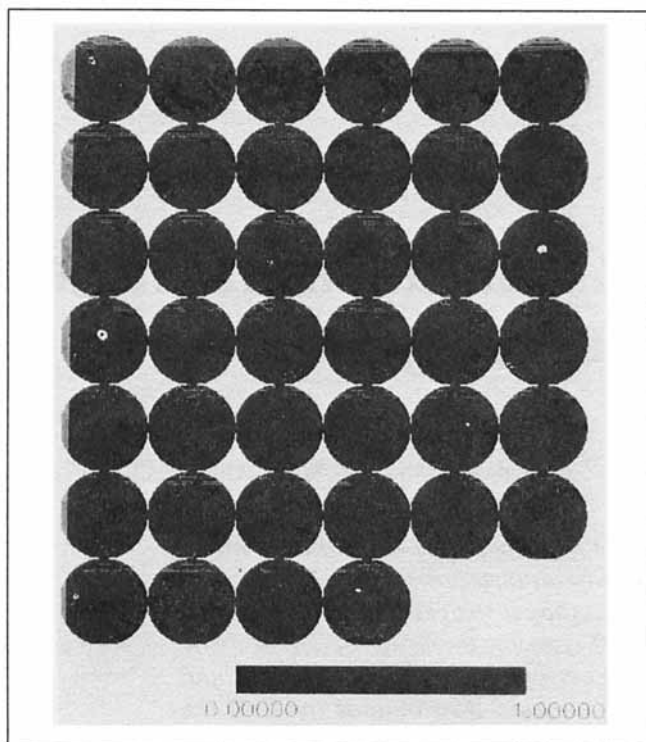


Figure 13. Water holdup image for a section of the trickle-bed column.

can be monitored as a function of inlet gas pressure, distributor design, and fluidization history. Use of particles tagged with NaI can be used as particle tracers. Even though the time of 3 s/frame is long for the observation of transient phenomena, use of multiple scans of the same section can provide input on the movement in the bed.

CAT scanning can be used for the quantitative evaluation of liquid and gas holdups in trickle beds. The holdups can be calculated easily using a linear model which combines scans of the bed dry, fully saturated with liquid and at trickle flow conditions.

## Acknowledgment

The author gratefully acknowledges Novacor Chemicals for permission to publish this article.

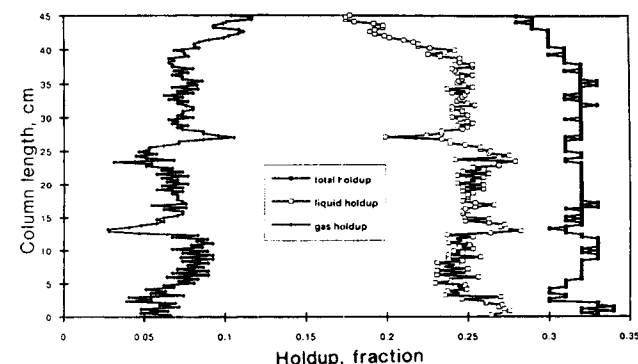


Figure 14. Average slice holdups for the trickle-bed column.

## Notation

- CT<sub>n</sub> = computer tomography number  
 $I$  = transmitted intensity (Bq)  
 $I_0$  = incident intensity (Bq)  
 $K$  = proportionality constant (500 or 1,000)  
 $L$  = path length (cm)

## Greek letters

- $\epsilon$  = holdup (fraction)  
 $\mu$  = linear attenuation coefficient (cm<sup>-1</sup>)  
 $\rho$  = density (g/cm<sup>3</sup>)

## Subscripts

- $g$  = gas  
 $l$  = liquid  
 (PE) = polyethylene  
 $\omega$  = water

## Literature Cited

- Bowman, J. D., "Use Column Scanning for Predictive Maintenance," *Chem. Eng. Prog.*, **87**(2), 25 (Feb., 1991).  
 Fincke, J. R., M. J. Berggren, and S. A. Johnson, "The Application of Reconstructive Tomography to the Measurement of Density Distribution in Two-Phase Flow," *Instrumentation in the Aerospace Industry*, p. 26; *Advances in Test Measurement*, p. 17; *Proc. Int. Instrumentation Symp.*, p. 235 (1980).  
 Kantzas, A., "Investigation of Physical Properties of Porous Rocks and Fluid Flow Phenomena in Porous Media Using Computer Assisted Tomography," *In Situ*, **14**(1), 77 (1990).  
 Kantzas, A., D. F. Marentette, and K. N. Jha, "Computer Assisted Tomography: From Qualitative Visualization to Quantitative Visualization to Quantitative Core Analysis," *J. Can. Pet. Techn.*, **31**(9), 48 (1992).  
 Lin, J. S., M. M. Chen, and B. T. Chao, "A Novel Radioactive Particle Tracking Facility for Measurement of Solids Motion in Gas Fluidized Beds," *AIChE J.*, **31**(3), 465 (Mar., 1985).  
 Lutran, P. G., K. M. Ng, and E. P. Delikat, "Liquid Distribution in Trickle Beds. An Experimental Study Using Computer Assisted Tomography," *Ind. Eng. Chem. Res.*, **30**, 1270 (1991).  
 MacCuaig, N., J. P. K. Seville, W. B. Gilboy, and R. Clift, "Application of Gamma-Ray Tomography to Gas Fluidized Beds," *Appl. Optics*, **24**(23), 4083 (1985).  
 Modi, V., C. Gnafakis, and C. C. Gryte, "X-Ray Computed Tomography of Horizontal Two Phase Pipe Flow," *Symp. NMR Imaging and CT Scanning for Multiphase Transport Processes*, AIChE Meeting (1990).  
 Ramachandran, P. A., and R. V. Chaudhari, "Three-Phase Catalytic Reactors," Gordon and Breach Science Publishers (1983).  
 Rowe, P. N., and R. Matsuno, "Single Bubbles Injected into a Gas Fluidized Bed and Observed by X-Rays," *Chem. Eng. Sci.*, **26**, 923 (1971).  
 Rowe, P. N., H. J. MacGillivray, and D. J. Cheesman, "Gas Discharge from an Orifice into a Gas Fluidized Bed," *Trans. I. Chem. E.*, **57**, 194 (1979).  
 Rowe, P. N., and H. J. MacGillivray, "The Structure of a 15 cm Diameter Gas Fluidized Bed Operated at up to 1 m/s and Seen by X-Rays," *Proc. Int. Fluidization Conf.*, J. R. Grace and J. M. Matsen, eds., p. 545 (1980).  
 Seville, J. P. K., J. E. P. Morgan, and R. Clift, "Tomographic Determination of the Voidage Structure of Gas Fluidized Beds in the Jet Region," *Proc. Eng. Found. Conf. Fluid.*, 5th ed., K. Oestergaard and A. Soerensen, eds., p. 87 (1986).  
 Vinegar, H. J., and S. L. Wellington, "Tomographic Imaging of Three-phase Flow Experiment," *Rev. Sci. Instrum.*, **58**(1), 96 (1987).  
 Yates, J. G., R. S. Ruiz-Martinez, and D. J. Cheesman, "Prediction of Bubble Size in a Fluidized Bed Containing Horizontal Tubes," *Chem. Eng. Sci.*, **45**(4), 105 (1990).

Manuscript received May 12, 1993, and revision received Sept. 28, 1993.